ACS APPLIED MATERIALS & INTERFACES

Forum Article

www.acsami.org

# Anisotropic Liquid Microcapsules from Biomimetic Self-Folding Polymer Films

Svetlana Zakharchenko and Leonid Ionov*

Leibniz Institute of Polymer Research Dresden, Hohe Strasse 6, D-01069 Dresden, Germany

**ABSTRACT:** We demonstrated a novel approach for the fabrication of anisotropic capsules with liquid content using biomimetic self-folding thermoresponsive polymer films. The behavior of self-folding films is very similar to actuation in plants, where nonhomogenous swelling results in complex movements such as twisting, bending, or folding. This approach allows the design of anisotropic liquid capsules with rodlike and dumbbell-like morphologies. We found that these capsules are able to assemble into different complex structures, such as nematic-like one and 3D network depending on their morphology.

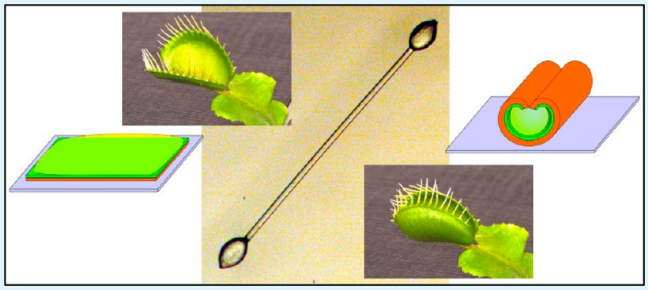

**KEYWORDS:** *polymer, actuator, self-folding, encapsulation, hydrogel*

## INTRODUCTION

Development of the methods for microencapsulation of liquids is a very important strategy for the design of self-healing materials,[1] regenerative medicine,[2] food industry,[3] etc. There are plenty of reports describing preparation of capsules[4,5] and particles with spherical shape. The anisotropic or elongated capsules are of a special interest, because the shape anisotropy gives them a number of advantages. For example, anisotropic capsules are particularly attractive for energy storage,[6] design of self-healing materials.[7] Anisotropy of delivery carriers is also a very desirable feature for pulmonary drug delivery because elongated carriers possess the same aerodynamic diameter as an equivalent spherical carrier, allowing at the same time for delivery of a larger amount of cargo.[8] Preparation of anisotropic liquid capsules is a far more challenging task, than synthesis of spherical capsules. Indeed, one needs to act against surface forces, which always compel liquid droplets to adopt spherical shape. There are several reports describing synthesis of aspherical capsules. For example, capsules with cubic and pyramid shapes were prepared using aspherical particles as a template that was covered by a polymer. Removal of the core led to a formation of an empty polymer shell with the shape defined by the template.[9−11] Anisotropic particles were also prepared using microfluidic nozzle system.[12] Recently, patterned surfaces were also applied for design of anisotropic capsules.[13]

One possible approach for the encapsulation is based on the use of self-folding films. Self-folding films are thin bilayers, which fold spontaneously in response to external stimuli in order to release internal stress[14−21] or external force.[22] The behavior of self-folding films is very similar to actuation in plants, where nonhomogenous swelling results in complex movements such as twisting, bending, or folding.[23,24] Such folding results in a transformation of 2D shapes into 3D objects, wherein the shape of the final object depends on many factors including the shape of the initial layout, the composition and thickness of the film, and the presence of hinges.[15,17,25−27] Recently, self-folding films were successfully applied for the encapsulation of solid hard and soft microobjects such as particles and cells.[14,28−30] In this paper, we report the fabrication of tubular capsules with liquid content using stimuli-responsive self-folding films.

## EXPERIMENTAL SECTION

**Materials.** Oleic acid (Fluka), cyclohexane 99.5% (Sigma-Aldrich), and rhodamine B (Sigma) were used as received. *N*-Isopropylacrylamide 97% (Aldrich), was recrystallized from hexane, methyl methacrylate 99% (Alrich) was purified by filtration through basic or neutral $Al_2O_3$ column before polymerization. Random copolymer of methyl methacrylate (MMA) and 4-acryloylbenzophenone (ABP), poly(methyl methacrylate-*co*-4-acryloyloxybenzophenone (1.6 mol %)) or p(MMA-ABP), was synthesized using free radical polymerization as described in ref 31. Random copolymer of *N*-isopropylacrylamide (NIPAM) and 4-acryloylbenzophenone (ABP), poly(*N*-isopropylacrylamide-*co*-4-acryloyloxybenzophenone ((1 mol %)) or p(NIPAM-ABP)), was synthesized using free radical polymerization as described in ref 29. Deionized (DI) water was obtained using TKA ultrapurification system (Germany), conductivity 0.055 $\mu$S/cm.

**Fabrication of Polymer Bilayers.** The bilayer films were fabricated by sequential deposition of P(NIPAM-ABP) and p(MMA-ABP) layers on a silicon substrate using dip-coating from ethanol and toluene solutions of the polymers, respectively. The thickness of polymer layers was 690 nm for PNIPAM-*co*-polymer and 70 nm for

**Special Issue:** Forum on Polymeric Nanostructures: Recent Advances toward Applications

**Received:** October 29, 2014
**Accepted:** January 21, 2015
**Published:** February 4, 2015




DOI: 10.1021/am505755j
*ACS Appl. Mater. Interfaces* 2015, 7, 12367−12372

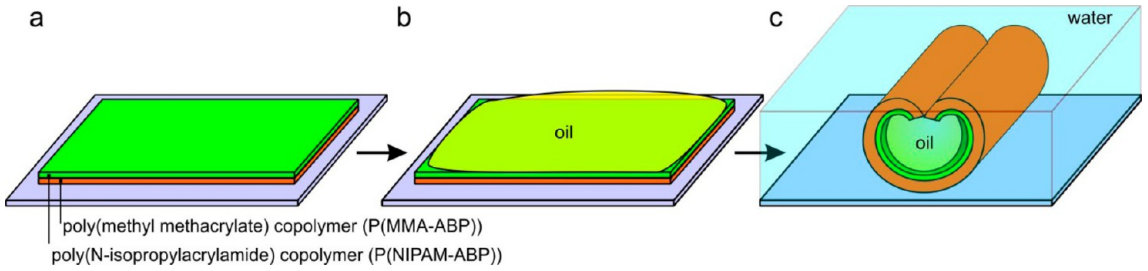


**Figure 1.** Scheme of the encapsulation of oily liquid into self-rolled polymer tubes in aqueous media: (a) prepared bilayer; (b) bilayer with deposited oil; (c) rolled bilayer tube with oil inside.

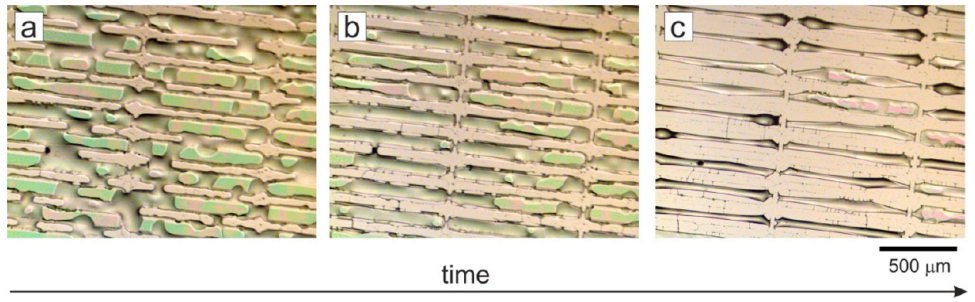


**Figure 2.** Time-resolved process of the encapsulation of oil inside self-rolled tubes: after (a) 20 s, (b) 80 s, and (c) 180 s of incubation in water at room temperature.

PMMA-copolymer. The polymer bilayers were patterned using contact photolithography. Samples were illuminated for 75 min using hand lamp (NH-15, Herolab, Germany) with the wavelengths of 254 nm. Irradiance at the sample to the lamp distance of 3 cm was ~330 $\mu$W/cm$^2$. The irradiation was performed through a photomask (Toppan Photomasks Inc., Germany) with rectangular patterns of the 126 $\mu$m × 1327 $\mu$m size. The irradiated film was rinsed with chloroform in order to remove non-cross-linked polymers leaving rectangular bilayer patterns.

**Deposition of Oleic Acid.** Oleic acid was deposited on the top of the patterned polymer bilayer using dip-coating. In order to adjust the thickness of the oil layer, mixtures of oleic acid with cyclohexane of the following volume ratios were used: 1:4, 1:3, 1:1, 3:1, and undiluted oleic acid. The thickness of the formed oil layer was estimated using the following equation

$$H_{\text{oleic acid}} = \frac{(m_2 - m_1)}{\rho a}$$

where $m_1$ and $m_2$ are the masses of the sample before and after oil deposition, respectively, $a$ is the area of the sample, and $\rho$ is the density of the oleic acid.

**Tube Formation and Oil Encapsulation.** Patterned bilayers were exposed in DI water at elevated temperature that was above LCST of PNIPAM-*co*-polymer (28 °C). Decreasing the temperature below LCST resulted in a formation of the tubes within 1−5 min and in a simultaneous encapsulation of the oil deposited on the top of the polymer bilayer.

## RESULTS AND DISCUSSION

In our approach for oil encapsulation, we used self-folding bilayers consisting of an active thermoresponsive poly(*N*-isopropylacrylamide)-copolymer (p(NIPAM-ABP)), and a passive hydrophobic poly(methyl methacrylate)-copolymer (p(MMA-ABP)). The photo-cross-linkable polymers containing benzophenone derivatives were sequentially deposited on a silica wafer using dip-coating from selective solvents, whereby active and passive polymers formed bottom and top layers, respectively (Figure 1a). The polymers were cross-linked by irradiation with UV light through a photomask. Finally, non-cross-linked polymers were removed by washing in a common solvent. As a result, an array of rectangular bilayer films was formed on the surface of the silicon wafer.

Oleic acid was deposited on the top of the patterned polymer bilayer using dip-coating from the mixtures of the oil with cyclohexane (Figure 1b). The dilution of oleic acid by the volatile solvent was performed in order to adjust the thickness of the deposited oil layer and, therefore, to vary the amount of the encapsulated oil. After deposition and evaporation of cyclohexane, oleic acid formed continuous film on the surface of the patterned bilayer. The oil film was stable in air at least for several minutes, but immediately started to dewet when immersed in water (Figure 2a, b). The oil left hydrophilic substrate areas between the bilayer patterns and covered the polymer areas because of the more favorable interaction with the top layer of the hydrophobic p(MMA-ABP). The thermoresponsive p(NIPAM-ABP) layer swelled when the temperature was decreased below the LCST of an active polymer that resulted in a folding of the polymer bilayer and in a formation of the tubular capsules with encapsulated oil (Figure 2c). The capsules could easily leave the surface of the wafer and go into an aqueous phase. Since the density of oleic acid (0.8 g/cm$^3$) is less than the density of water (1 g/cm$^3$), one can expect that oil droplets can separate from the polymer surface and float on the water surface. Interestingly, we didn't observe this effect, most probably because the buoyancy acting on oil droplet ($F = \rho_{\text{water}} V_{\text{oleicacid}} g = 1 \times 10^{-7}$ N) is much smaller than surface forces ($F \approx l_{\text{pattern}} + w_{\text{pattern}})\gamma_{\text{oleicacid}} \approx 1 \times 10^{-5}$ to $1 \times 10^{-4}$ N.

The swelling of the p(NIPAM-BA) films is a reversible process and the cycles of swelling and shrinking can be repeated many times in a reproducible manner, influencing the rolling behavior of the bilayer films. Indeed, empty self-rolled tubes, based on this polymer, demonstrate clear reversibility of folding in response to the temperature.[29] Interestingly, we observed almost no thermoresponsive behavior of the PNIPAM-based tubes with encapsulated oleic acid. In this


DOI: 10.1021/am505755j
ACS Appl. Mater. Interfaces 2015, 7, 12367−12372

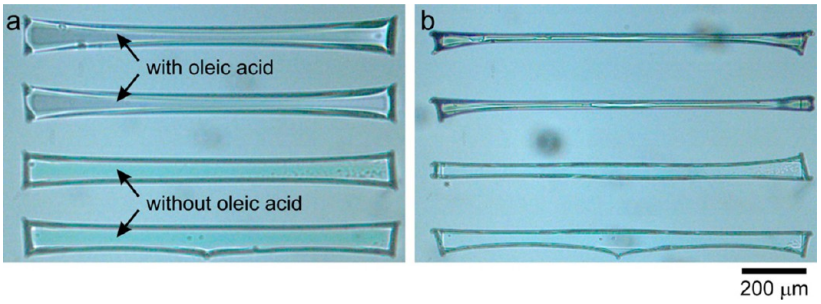


**Figure 3.** Optical microscopy snapshots of rolling of polymer bilayers with oleic acid and without it after (a) 10 s and (b) 20 s of rolling.

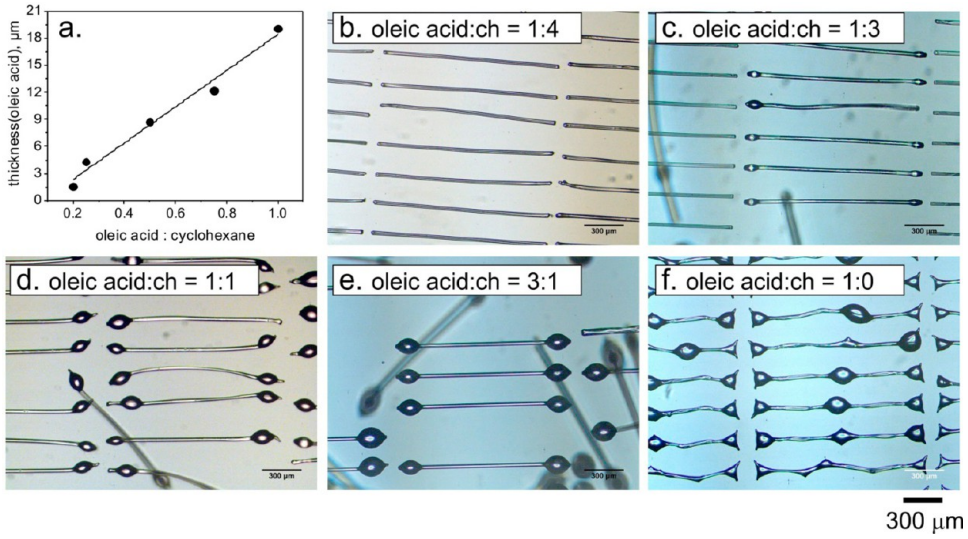


**Figure 4.** Tubular self-rolled capsules with encapsulated oleic acid: (a) thickness of the film of oleic acid on the surface of patterned bilayer depending on the volume ratio of oleic acid and cyclohexane; (b–f) optical microscopy images of capsules with oleic acid obtained by rolling of polymer bilayer with different thickness of oleic acid, which is determined by ratio between oleic acid and cyclohexane (ch).

case, tubes slightly decrease and increase their diameter upon cooling and heating, respectively, but no unfolding of the tubes occurs at the temperatures above the LCST of the PNIPAM-copolymer. The difference in responsive behavior between empty and oil-filled tubes can be explained by considering the acting forces: unfolding of the oil-filled tube would require an increase in the contact area between oleic acid and water that is energetically unfavorable. Surface force acting on droplet with the size of bilayer pattern is of order of magnitude $F \approx (l_{pattern} + w_{pattern})\gamma_{oleicacid} \approx 1 \times 10^{-5}$ to $1 \times 10^{-4}$ N. Force generated during unfolding of the film was estimated in consideration that rolling of the bilayer occurs along its long side and the moment of inertia of the bilayer ($I_{bilayer} = l_{pattern}h^3_{bilayer}/12 \approx 1 \times 10^{-22}$ $m^4$ is independent of the width of the bilayer. In the order of magnitude of this force $F \approx d_{tube}EI_{bilayer}/w^3_{pattern} \approx (1 \times 10^{-5}$ (m))$(1 \times 10^{-22}$ ($m^4$))$(1 \times 10^8$ ($N/m^2$))/$(1 \times 10^{-12}$ ($m^3$)) $\approx 1 \times 10^{-4}$ N is comparable with the surface forces or slightly exceed them.

One can assume that the final diameter of the tube must be dependent on the amount of deposited oleic acid if surface tension forces dominate. On the other hand, the experimental observations demonstrate that the diameter of the tubes is independent of the thickness of deposited oleic acid and remains ca. 10 $\mu$m (Figures 3 and 4). Moreover, rolling expels oleic acid from the inner of the tube that results in a formation of droplets. These observations indicate domination of the forces generated by the swelling of the active hydrogel. We also investigated the effect of oleic acid on the tube formation by observing films with deposited oleic acid and without it (Figure 3). It was found that rolling without oleic acid is slower and inhomogenous, i.e., narrow tubes are formed along the perimeter of the film, whereas its center remains undeformed. The rolling of the films with oleic acid is faster (diameter of tubes decreases faster) and more homogeneous, i.e., periphery of the film and its central part deform simultaneously. Since the rolling in the presence of oleic acid is faster, we can assume that surface tension affects folding behavior. Thus, experimental observations indicate that surface tension, forces generated by the swelling hydrogel and elastic force generated by the PMMA layer play considerable role during the folding. In multilayer films, there are other forces such as adhesion of the thermoresponsive layer to the substrate and adhesion of the polymer layers to each other when multilayer films are formed. The last force, for example, prevents unrolling of the films.[29] This diversity of the forces acting on the films makes elucidation of the contribution of each of them very difficult.

We found that morphology of the formed capsules was determined by the amount of oleic acid deposited on the bilayer. The thickness of the film formed by oleic acid after evaporation of the solvent decreased with the increase in the dilution degree (Figure 4a). We observed that all available oil was encapsulated entirely within the inner volume of the tubes and no droplets outside (dumbbell-like shapes) were formed when the thinnest layer of oleic acid was used (Figure 4b).


DOI: 10.1021/am505755j
ACS Appl. Mater. Interfaces 2015, 7, 12367–12372

Increase in the thickness of the oil layer led to its excess compared to the available volume of the capsules. As a result, excess of the oil formed the droplets at both ends of the tubes, i.e., dumbbell-like capsules were formed. The size of these droplets increased with the increase of the excess of the oil (Figure 4c–e). Finally, use of undiluted oleic acid for the deposition resulted in a formation of three droplets along the capsule: two at the ends of the tube and one in the center (Figure 4f). Transition from a two-droplet case to a three-droplet case is not completely clear. In fact, formation of one droplet instead of two or three is always more energetically favorable because of lower interfacial energy. Therefore, we assume that formation of three droplets has kinetic character and is due to the high viscosity of oil that does not have sufficient time to move to one of the ends during rolling.

The obtained microcapsules (Figure 4d, e) consist of a cylindrical part, which is polymer bilayer tube with encapsulated oil, two droplets at the ends of the tube. These droplets are liquid but their surface can potentially be solidified by using surface polymerization initiated in water phase that is very close to the approach used for the preparation of spherical capsules for self-healing materials.[32] In fact, capsules with liquid content are widely used for the design of self-healing materials. The disadvantage of spherical particles is that they can be used only once. More promising is the use of vascular networks, which provide a permanent supply of healing agents even to the place that was already healed many times.[33] Tubes with liquid content could be the elements of such networks.

We found that crystallization of oleic acid ($T_m$ = 13–14 °C) in the capsules is inhomogeneous: molten oleic acid (Figure 5a) crystallizes first in the side droplets (Figure 4b) and then

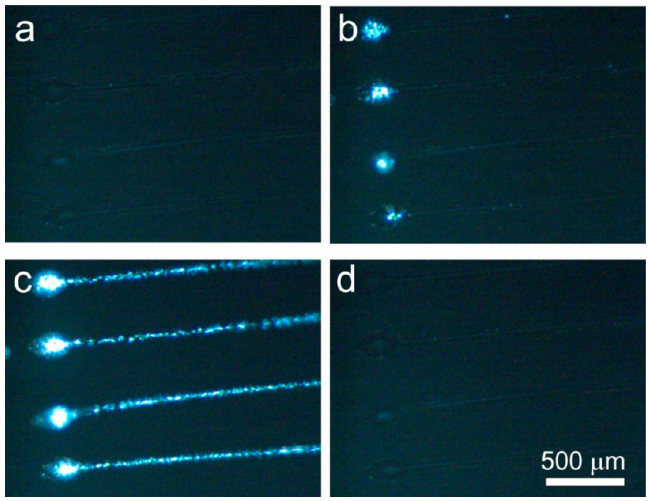


**Figure 5.** Optical dark-field microscopy images of crystallization and melting of oleic acid inside the folded capsules: (a) molten oleic acid ($T$ = 20 °C); (b) after start of crystallization in side droplets ($T$ = 11 °C); (c) after start of crystallization in tubes ($T$ = 11 °C); (d) after melting of crystallized oleic acid ($T$ = 20 °C).

inside the tubes (Figure 5c). Contrary, melting of the crystallized oleic acid occurs simultaneously in the side droplets and inside the tube (Figure 5d). We believe that the reason for delayed crystallization inside the tubes is the confinement effect—walls of the tubes restrict growth of crystals of oleic acid. The walls do not, however, affect melting of the crystals and the melting occurs simultaneously inside the tubes and in side droplets.

Finally, we investigated interactions between oil-filled capsules. The capsules that had large side droplets spontaneously stuck to each other because of the merging of the side oil droplets (Figure 6a–d). The merging oil droplets formed

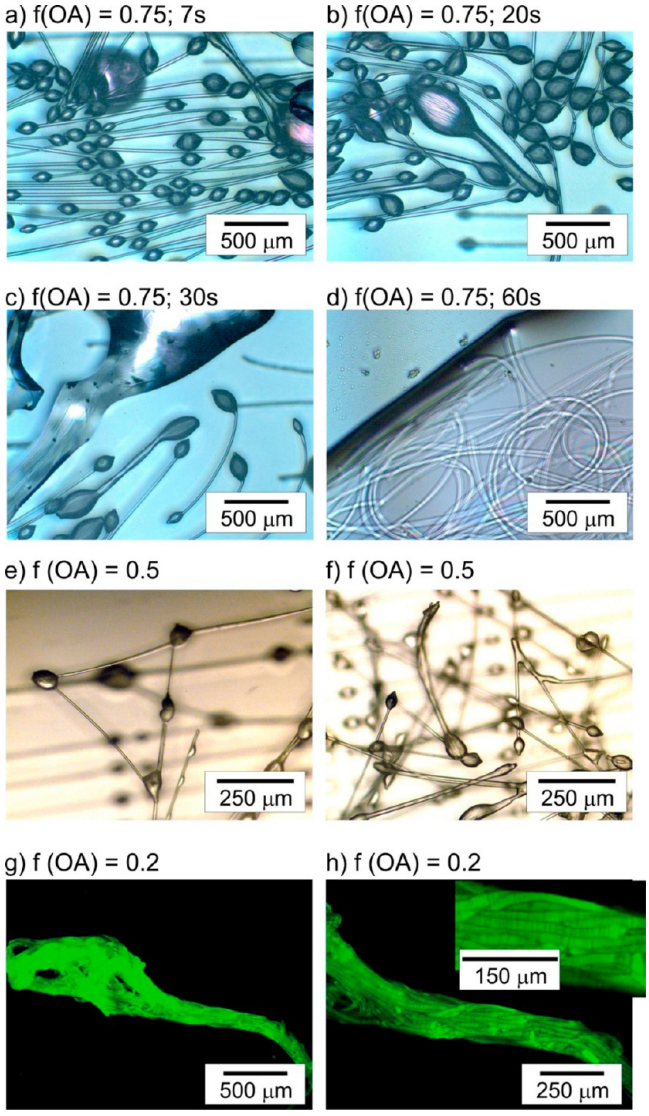


**Figure 6.** Self-assembly of oil-filled tubes in water depending on the amount of encapsulated oil. Volume fraction of oleic acid during deposition, f(OA) = Voleicacid:(Voleicacid + Vcyclohexane): (a) f(OA) = 0.75, 7 s after rolling; (b) f(OA) = 0.75, 20 s after rolling; (c) f(OA) = 0.75, 30 s after rolling; (d) f(OA) = 0.75, 60 s after rolling; (e, f) f(OA) = 0.5; (g, h) f(OA) = 0.2, after assembly of the tubes in aqueous media upon mechanical agitation (green fluorescence is due to Rhodamine B dissolved in oleic acid).

larger ones until very large oil droplets with tubes inside were formed (Figure 6d). The assembly of the capsules, which contained oil only inside, occurred slowly when tubes were rinsed from the substrate into a glass vial and mechanical agitation was applied. Under these conditions, tubes started to stick to each other because of a small leakage of oil. The capsules thus formed tight bundles where capsules were oriented in one direction (Figure 6g,h). The orientation of capsules in such aggregate is similar to the structure of nematic liquid crystals. Interactions of the capsules having the side oil droplets of the moderate size had a particularly interesting


DOI: 10.1021/am505755j
ACS Appl. Mater. Interfaces 2015, 7, 12367–12372

character. (Figure 6e, f). In this case, the capsules assembled in a complex way and formed chains and network knots that is very similar to behavior of rods, which can stick to each other by their ends.[34] The capsules stick to each other by their oily heads forming long agglomerates, which finally build a 3D network.

## CONCLUSIONS

In this paper, we demonstrated a novel approach for the fabrication of anisotropic capsules with liquid content using self-folding films. This approach allows the design of anisotropic capsules with different morphology such as rodlike and dumbbell-like. We found that these capsules are able to assemble into different complex nematic-like structures and 3D networks. There are several reports describing fabrication of macroscopic self-folded capsules using capillary forces generated by encapsulated droplets.[22,35,36] Such capsules form when a droplet is deposited in onthe film and unfold when the droplet evaporates. In our approach, the smaller capsules are formed due to the swelling of one of the components of the film and remain folded even if the encapsulated material is removed. We foresee great potential of the demonstrated approach for the design of microfluidic networks, self-healing materials, and drug delivery.

## AUTHOR INFORMATION

### Corresponding Author

*E-mail: ionov@ipfdd.de.

### Funding

DFG (IO 68/1−1)

### Notes

The authors declare no competing financial interest.

## REFERENCES

(1) Yang, Y.; Urban, M. W. Self-Healing Polymeric Materials. *Chem. Soc. Rev.* **2013**, *42*, 7446−7467.
(2) Pedraz, J. L.; Hernandez, R. M.; Orive, G.; Murua, A. Microcapsules and Microcarriers for in Situ Cell Delivery. *Adv. Drug Delivery Rev.* **2010**, *62*, 711−730.
(3) Anal, A. K.; Singh, H. Recent Advances in Microencapsulation of Probiotics for Industrial Applications and Targeted Delivery. *Trends Food Sci. Technol.* **2007**, *18*, 240−251.
(4) Yow, H. N.; Routh, A. F. Formation of Liquid Core−Polymer Shell Microcapsules. *Soft Matter* **2006**, *2*, 940−949.
(5) Scott, C.; Wu, D.; Ho, C.-C.; Co, C. C. Liquid-Core Capsules via Interfacial Polymerization: A Free-Radical Analogy of the Nylon Rope Trick. *J. Am. Chem. Soc.* **2005**, *127*, 4160−4161.
(6) Liu, J.; Xia, H.; Lu, L.; Xue, D. Anisotropic $Co_3O_4$ Porous Nanocapsules toward High-Capacity Li-Ion Batteries. *J. Mater. Chem.* **2010**, *20*, 1506−1510.
(7) Van Tittelboom, K.; De Belie, N.; Van Loo, D.; Jacobs, P. Self-Healing Efficiency of Cementitious Materials Containing Tubular Capsules Filled with Healing Agent. *Cement Concrete Comp.* **2011**, *33*, 497−505.
(8) Chow, A. L.; Tong, H. Y.; Chattopadhyay, P.; Shekunov, B. Particle Engineering for Pulmonary Drug Delivery. *Pharm. Res.* **2007**, *24*, 411−437.
(9) Shchepelina, O.; Kozlovskaya, V.; Kharlampieva, E.; Mao, W.; Alexeev, A.; Tsukruk, V. V. Anisotropic Micro- and Nano-Capsules. *Macromol. Rapid Commun.* **2010**, *31*, 2041−2046.
(10) Holt, B.; Lam, R.; Meldrum, F. C.; Stoyanov, S. D.; Paunov, V. N. Anisotropic Nano-papier Mache Microcapsules. *Soft Matter* **2007**, *3*, 188−190.
(11) Kozlovskaya, V.; Wang, Y.; Higgins, W.; Chen, J.; Chen, Y.; Kharlampieva, E. pH-Triggered Shape Response of Cubical Ultrathin Hydrogel Capsules. *Soft Matter* **2012**, *8*, 9828−9839.
(12) Sugiura, S.; Oda, T.; Aoyagi, Y.; Satake, M.; Ohkohchi, N.; Nakajima, M. Tubular Gel Fabrication and Cell Encapsulation in Laminar Flow Stream Formed by Microfabricated Nozzle Array. *Lab Chip* **2008**, *8*, 1255−1257.
(13) Ye, C.; Kulkarni, D. D.; Dai, H.; Tsukruk, V. V. Programmable Arrays of "Micro-Bubble" Constructs via Self-Encapsulation. *Adv. Funct. Mater.* **2014**, *24*, 4364−4373.
(14) Stroganov, V.; Zakharchenko, S.; Sperling, E.; Meyer, A. K.; Schmidt, O. G.; Ionov, L. Biodegradable Self-Folding Polymer Films with Controlled Thermo-Triggered Folding. *Adv. Funct. Mater.* **2014**, *24*, 4357−4363.
(15) Thérien-Aubin, H.; Wu, Z. L.; Nie, Z.; Kumacheva, E. Multiple Shape Transformations of Composite Hydrogel Sheets. *J. Am. Chem. Soc.* **2013**, *135*, 4834−4839.
(16) Leong, T. G.; Randall, C. L.; Benson, B. R.; Zarafshar, A. M.; Gracias, D. H. Self-Loading Lithographically Structured Microcontainers: 3D Patterned, Mobile Microwells. *Lab Chip* **2008**, *8*, 1621−1624.
(17) Kim, J.; Hanna, J. A.; Byun, M.; Santangelo, C. D.; Hayward, R. C. Designing Responsive Buckled Surfaces by Halftone Gel Lithography. *Science* **2012**, *335*, 1201−1205.
(18) Yuan, B.; Jin, Y.; Sun, Y.; Wang, D.; Sun, J.; Wang, Z.; Zhang, W.; Jiang, X. A Strategy for Depositing Different Types of Cells in Three Dimensions to Mimic Tubular Structures in Tissues. *Adv. Mater.* **2012**, *24*, 890−896.
(19) He, H. Y.; Guan, J. J.; Lee, J. L. An Oral Delivery Device Based on Self-Folding Hydrogels. *J. Controlled Release* **2006**, *110*, 339−346.
(20) Shim, T. S.; Kim, S.-H.; Heo, C.-J.; Jeon, H. C.; Yang, S.-M. Controlled Origami Folding of Hydrogel Bilayers with Sustained Reversibility for Robust Microcarriers. *Angew. Chem., Int. Ed.* **2012**, *51*, 1420−1423.
(21) Smela, E.; Inganas, O.; Lundstrom, I. Controlled Folding of Micrometer-Size Structures. *Science* **1995**, *268*, 1735−1738.
(22) Py, C.; Reverdy, P.; Doppler, L.; Bico, J.; Roman, B.; Baroud, C. N. Capillary Origami: Spontaneous Wrapping of a Droplet with an Elastic Sheet. *Phys. Rev. Lett.* **2007**, *98*, 156103.
(23) Ionov, L. Biomimetic Hydrogel-Based Actuating Systems. *Adv. Funct. Mater.* **2013**, *23*, 4555−4570.
(24) Fratzl, P.; Barth, F. G. Biomaterial Systems for Mechanosensing and Actuation. *Nature* **2009**, *462*, 442−448.
(25) Gracias, D. H. Stimuli Responsive Self-Folding Using Thin Polymer Films. *Curr. Opin Chem. Eng.* **2013**, *2*, 112−119.
(26) Stoychev, G.; Turcaud, S.; Dunlop, J. W. C.; Ionov, L. Hierarchical Multi-step Folding of Polymer Bilayers. *Adv. Funct. Mater.* **2013**, *23*, 2295−2300.
(27) Azam, A.; Laflin, K. E.; Jamal, M.; Fernandes, R.; Gracias, D. H. Self-Folding Micropatterned Polymeric Containers. *Biomed. Microdevices* **2011**, *13*, 51−58.
(28) Zakharchenko, S.; Puretskiy, N.; Stoychev, G.; Waurisch, C.; Hickey, S. G.; Eychmuller, A.; Sommer, J.-U.; Ionov, L. Stimuli-Responsive Hierarchically Self-Assembled 3D Porous Polymer-Based Structures with Aligned Pores. *J. Mater. Chem. B* **2013**, *1*, 1786−1793.
(29) Zakharchenko, S.; Puretskiy, N.; Stoychev, G.; Stamm, M.; Ionov, L. Temperature Controlled Encapsulation and Release Using Partially Biodegradable Thermo-magneto-sensitive Self-Rolling Tubes. *Soft Matter* **2010**, *6*, 2633−2636.
(30) Stoychev, G.; Puretskiy, N.; Ionov, L. Self-Folding All-Polymer Thermoresponsive Microcapsules. *Soft Matter* **2011**, *7*, 3277−3279.
(31) Stoychev, G.; Zakharchenko, S.; Turcaud, S.; Dunlop, J. W. C.; Ionov, L. Shape Programmed Folding of Stimuli-Responsive Polymer Bilayers. *ACS Nano* **2012**, *6*, 3925−3934.
(32) Blaiszik, B. J.; Sottos, N. R.; White, S. R. Nanocapsules for Self-Healing Materials. *Compos. Sci. Technol.* **2008**, *68*, 978−986.
(33) Toohey, K. S.; Sottos, N. R.; Lewis, J. A.; Moore, J. S.; White, S. R. Self-healing materials with microvascular networks. *Nat. Mater.* **2007**, *6*, 581−585.


DOI: 10.1021/am505755j
*ACS Appl. Mater. Interfaces* 2015, 7, 12367−12372

(34) Gu, Z.; Chen, Y.; Gracias, D. H. Surface Tension Driven Self-Assembly of Bundles and Networks of 200 nm Diameter Rods Using a Polymerizable Adhesive. *Langmuir* **2004**, *20*, 11308−11311.
(35) Mirsaidov, U.; Mokkapati, V. R. S. S.; Bhattacharya, D.; Andersen, H.; Bosman, M.; Ozyilmaz, B.; Matsudaira, P. Scrolling Graphene into Nanofluidic Channels. *Lab Chip* **2013**, *13*, 2874−2878.
(36) Pineirua, M.; Bico, J.; Roman, B. Capillary Origami Controlled by an Electric Field. *Soft Matter* **2010**, *6*, 4491−4496.


DOI: 10.1021/am505755j
*ACS Appl. Mater. Interfaces* 2015, 7, 12367−12372